

A Kinetic Model for Enzyme Interfacial Activity and Stability: *pa*-Hydroxynitrile Lyase at the Diisopropyl Ether/Water Interface

Luis G. Cascão Pereira,¹ Andrea Hickel,² Clayton J. Radke,¹ Harvey W. Blanch¹

¹Department of Chemical Engineering, University of California, Berkeley, California 94720-1462; telephone: 510-642-5204; 510-642-1387; fax: 510-642-4778; e-mail: radke@cchem.berkeley.edu; blanch@cchem.berkeley.edu

²Institut für Biophysik und Röntgenstrukturforschung, OEAW Schmiedlstrasse 6, 8042, Graz, Austria

Received 15 October 2001; accepted 18 December 2001

DOI: 10.1002/bit.10241

Abstract: A kinetic framework is developed to describe enzyme activity and stability in two-phase liquid–liquid systems. In particular, the model is applied to the enzymatic production of benzaldehyde from mandelonitrile by *Prunus amygdalus* hydroxynitrile lyase (*pa*-Hnl) adsorbed at the diisopropyl ether (DIPE)/aqueous buffer interface (pH = 5.5). We quantitatively describe our previously obtained experimental kinetic results (Hickel et al., 1999; 2001), and we successfully account for the aqueous-phase enzyme concentration dependence of product formation rates and the observed reaction rates at early times. Multilayer growth explains the early time reversibility of enzyme adsorption at the DIPE/buffer interface observed by both enzyme-activity and dynamic-interfacial-tension washout experiments that replace the aqueous enzyme solution with a buffer solution. The postulated explanation for the unusual stability of *pa*-Hnl adsorbed at the DIPE/buffer interface is attributed to a two-layer adsorption mechanism. In the first layer, slow conformational change from the native state leads to irreversible attachment and partial loss of catalytic activity. In the second layer, *pa*-Hnl is reversibly adsorbed without loss in catalytic activity. The measured catalytic activity is the combined effect of the deactivation kinetics of the first layer and of the adsorption kinetics of each layer. For the specific case of *pa*-Hnl adsorbed at the DIPE/buffer interface, this combined effect is nearly constant for several hours resulting in no apparent loss of catalytic activity. Our proposed kinetic model can be extended to other interfacially active enzymes and other organic solvents. Finally, we indicate how interfacial-tension lag times provide a powerful tool for rational solvent selection and enzyme engineering. © 2002 Wiley Periodicals, Inc. *Biotechnol Bioeng* 78: 595–605, 2002.

Keywords: hydroxynitrile lyase; interfacial enzyme catalysis; two-phase systems; dynamic-tension lag time; kinetic model

INTRODUCTION

Adsorption of proteins at fluid and solid interfaces, accompanied by conformational changes that may impact their catalytic or biological function, is of importance for a wide range of applications, including industrial biocatalysis, and delivery and stabilization of therapeutic proteins. With an increasing number of therapeutic proteins reaching commercialization, novel delivery routes are needed to transport large molecular-weight compounds through the human body while retaining efficacy and stability (Malmsten, 1998; Park and Mrsny, 2000). Delivery routes include transport across interfaces involved in pulmonary drug delivery, transdermal patches, and electrotransport. Enzymes are also increasingly finding application as biotransformation agents in two-phase liquid systems. One of the main obstacles precluding wider use of enzymes as industrial biocatalysts is the lack of understanding of their adsorption behavior and possible conformational changes leading to denaturation at liquid/liquid and gas/liquid interfaces.

In this work, we present a framework for the analysis of interfacial enzymatic reactions in two-phase liquid–liquid systems. The approach is based on understanding obtained from our earlier experimental studies employing hydroxynitrile lyase from *Prunus amygdalus* (*pa*-Hnl, EC 4.1.2.10) adsorbed at the organic solvent/water interface (Hickel et al., 1998; 1999; 2001). Because of their usefulness in the formation and cleavage of chiral cyanohydrins, Hnls are potentially valuable biocatalysts for the chemical industry (Dreveny et al., 2001; Effenberger, 1994; Effenberger et al., 2000; Johnson et al., 2000; Wajant and Effenberger, 1996). Challenges in the application of Hnls at an industrial scale, however, include the aqueous-phase chemical reaction leading to a decrease in product enantiomeric purity, bulk enzyme

Correspondence to: C. J. Radke, H. W. Blanch

Contract grant sponsors: Department of Energy (grant DE-FG03-94ER14456); Nestlé Inc., Switzerland

instability at low pH values, and the lack of availability of enzyme in large amounts (Hickel and Griengl, 1996; Hickel et al., 1997). Using the enzymes in an organic/aqueous two-phase system, where the substrate and product are primarily soluble in the organic phase, could potentially solve some of these problems. Here, the aqueous-phase background reaction is negligible, and the enzymes can be used at pH values near their stability and activity optima. (Bauer et al., 1999; Effenberger, 1994; Förster et al., 1996; Loos et al., 1995).

Previously, we established that mandelonitrile cleavage to form benzaldehyde by pa-Hnl is carried out by the enzyme residing directly (i.e., adsorbed) at the organic solvent/water interface and does not result from activity in the bulk aqueous phase (Hickel et al., 1999). pa-Hnl exhibits the highest stability but the lowest initial catalytic activity at the aqueous/organic solvent interface with highly polar organic solvents. Thus, use of diisopropylether (DIPE) and methyl tert-butyl ether (MTBE) results in no loss in enzyme activity over a period of several hours. Conversely, the more apolar the solvent, the higher is the initial pa-Hnl catalytic activity, and the more rapid is the loss of activity, as is evidenced by heptane and dibutyl-ether (DBE) kinetic data. pa-Hnl adsorbs irreversibly after 30 min at the DIPE/water interface, but with no apparent loss of catalytic activity (Hickel et al., 2001). Dynamic-interfacial-tension measurements indicate that pa-Hnl adsorbs more strongly at the interface of apolar solvents. This is attributed to a higher number of molecular contacts with the interface due to enzyme unfolding and denaturing following adsorption (Hickel et al., 1998).

In this work, we develop a quantitative kinetic model for enzyme adsorption at the organic solvent/water interface, which sequentially results in denaturation. Thus, following adsorption at the interface, enzyme conformational changes lead to a reduction in catalytic activity. We describe interfacial denaturation by a simplified two-state process: the enzyme assumes native (N) and unfolded (U) conformations. Multilayer growth is described by incorporation of a second enzyme layer at the interface. The model is applied here to the cleavage of mandelonitrile to benzaldehyde by pa-Hnl at the DIPE/water interface at pH 5.5 in a phosphate buffer.

Previous kinetic models for the reaction catalyzed by pa-Hnl in two-phase systems fail to account for the interfacial nature of the reaction (Willeman et al., 2000). Specifically, the model presented here correctly portrays the observed partial reversibility of enzyme adsorption at long times, the constant reaction rates observed at early times, and the reaction-rate dependence on bulk enzyme concentration. Our kinetic framework can be easily extended to other enzymes and to other organic solvents.

In addition, the proposed model provides a rationale for the observed differences in interfacial-tension lag times upon pa-Hnl adsorption at different organic sol-

vent/water interfaces. Deviations of the lag times from those based on mass-transfer resistances indicate the existence of important interfacial adsorption and unfolding barriers with implications for the maintenance of catalytic activity over long reaction times.

Observed Kinetics of pa-Hnl at the DIPE/Water Interface

An example of interfacial enzyme kinetics is provided by the measured cleavage kinetics of mandelonitrile to benzaldehyde by *pa-Hydroxynitrile lyase* at an organic solvent/water interface from Hickel et al. (1998; 1999; 2001). We focus here primarily on the DIPE/water interface at pH 5.5, which represents a promising organic solvent/aqueous solution combination for two-phase catalysis with pa-Hnl (Hickel et al., 1999; Kiljunen and Kanerva, 1997a; 1997b). The kinetics of this interfacial reaction is available as a function of time, bulk enzyme concentration, nature of the organic phase, and enzyme adsorption in a recycle-reactor with no mass-transfer limitations in either the organic or aqueous phases. We briefly review the experimental findings and their current interpretation.

Hickel et al. (1999) established for the first time that pa-Hnl residing at the organic solvent/water interface is responsible for mandelonitrile cleavage. Evidence for an interfacial reaction included a linear dependence of the reaction rate on interfacial area, no dependence on the aqueous-phase volume, and cessation of the reaction when the interface is preadsorbed with denatured enzyme. Details are provided elsewhere (Hickel et al., 1999).

pa-Hnl exhibits high stability but low initial catalytic activity at the aqueous-organic interface with polar solvents, such as DIPE. In contrast, pa-Hnl adsorption at the apolar heptane/water interface initiates a burst in kinetic activity followed by complete deactivation within minutes. However, no loss in activity is observed for several hours with DIPE as the organic solvent (Hickel et al., 2001). In parallel with these observations, dynamic-surface-tension measurements at both interfaces for the same enzyme concentration indicates rapid interfacial-tension lowering at the heptane/water interface, while no appreciable interfacial tension lowering is obtained for several hours with DIPE as the organic solvent (Hickel et al., 2001). These observations were explained on the basis of a higher degree of unfolding at the more apolar organic/water interfaces (i.e., heptane/water) leading to loss of enzymatic activity.

pa-Hnl at the DIPE/water interface follows Michaelis-Menten kinetics, where, additionally, a small amount of substrate appears necessary for enzyme activation (Hickel et al., 1999). Even though adsorbed to the DIPE/water interface, pa-Hnl displays remarkable stability, as indicated by constant reaction rates for up to several hours. This finding is illustrated by the open

symbols in Figure 1 where for several aqueous enzyme concentrations, a linear dependence of product concentration on time reflects constant reaction rates. Solid lines in this figure, and in Figures 2 and 3 to follow, correspond to theory and are described later. At high aqueous enzyme concentrations, the observed enzymatic activity reaches a plateau, as indicated by the closed circles in Figure 2, characteristic of an adsorption-packing limitation.

The results shown in Figures 1 and 2 were previously interpreted by postulating reversible Langmuir adsorption at the interface (Hickel et al., 1999). However, later washout data obtained by replacing the aqueous enzyme solution with a buffer solution indicate that pa-Hnl is partially irreversibly adsorbed after only 30 min of exposure to the interface (Hickel et al., 2001). For example, the closed circles in Figure 3 reveal that after the enzyme has been adsorbed at the interface for more than 180 min the remaining activity after washout of the aqueous enzyme is about one third of the initial value. However, dynamic interfacial-tension measurements done under similar conditions demonstrate complete irreversibility on this time scale (cf., Figs. 9–11 of Hickel et al., 2001). Based on these results, Hickel et al. (2001) proposed either that about one third of the enzyme is irreversibly adsorbed and retains its initial catalytic activity or that a second adsorbed layer augments the

overall measured catalytic activity without contributing to surface-tension lowering.

In the next sections, we develop a kinetic framework for interfacial enzymatic reactions. Within this framework, we reconcile our earlier results (Hickel et al., 1999) with our most recent observations (Hickel et al., 2001). Specifically, we account for the observed partial reversibility of enzyme adsorption, as determined from enzyme-activity washout experiments, the total irreversibility of adsorption observed in dynamic interfacial-tension experiments, the reaction-rate dependence with bulk enzyme concentration, and the apparent constant rates of reaction observed at early times. In addition, we provide a quantitative interpretation of dynamic interfacial-tension measurements and describe their usefulness in predicting enzyme stability at different organic solvent/water interfaces.

A Model for Interfacial Enzyme Adsorption and Activity

Proteins have long been known to adsorb strongly at interfaces (Stuart et al., 1991). Upon adsorption from the aqueous phase, proteins may undergo significant conformational changes in an attempt to lower their interfacial free energy by exposure and even protrusion of hydrophobic segments into an air or organic phase.

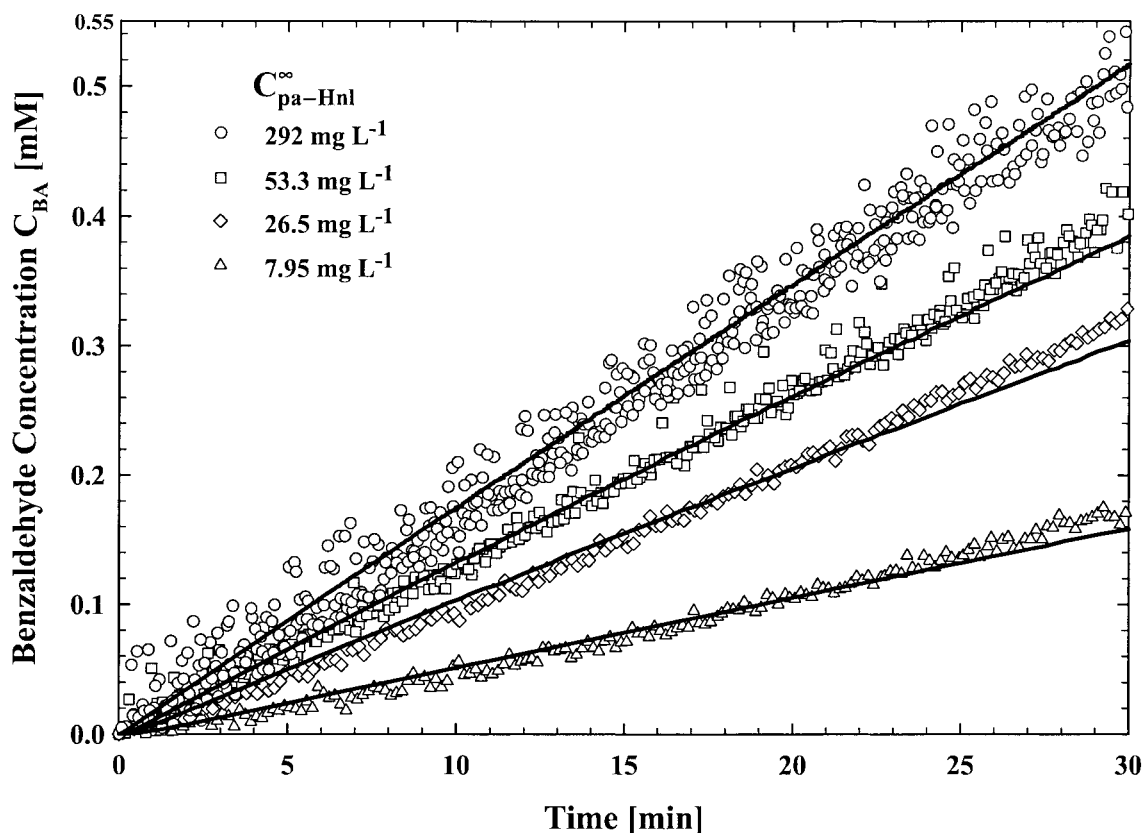


Figure 1. Dependence of benzaldehyde product formation, ($C_{BA} = P$), on time different enzyme concentrations: 50 mM KH_2PO_4 , pH 5.5, $C_{MN} = 10.1$ mM. The solid lines are a best fit to the kinetic model in Equations (1)–(4).

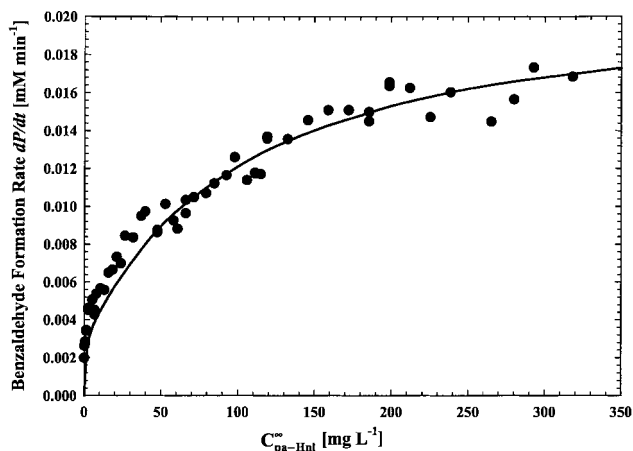


Figure 2. Interfacial benzaldehyde product formation rate, dP/dt , as a function of the aqueous-phase pa-Hnl concentration. The solid line corresponds to a best fit to the kinetic model in Equations (1)–(4) with $S = C_{MN} = 10.1 \text{ mM}$, $S_0 = 1.33 \text{ mM}$, $K_M = 14.4 \text{ mM}$, $50 \text{ mM KH}_2\text{PO}_4$ buffer, pH 5.5. After Hickel et al. (1999) with permission.

Although there are few reports providing direct observations of conformational changes (see, however, Tupy, 1998), such changes are evidenced by enzyme deactivation upon exposure to an interface, interfacial-tension lowering over long periods of time, multilayer growth, and development of interfacial networks, such as skins (Cascão Pereira et al., 2001; Graham and Phillips, 1979a; Tupy et al., 1998). Adsorbed proteins may be present in various conformational states with different degrees of unfolding that result in differences in enzymatic activity, ranging from fully active to inactive. The presence of various unfolded interfacial conformations corresponds to current descriptions of enzyme deactivation in bulk water resulting from denaturing agents

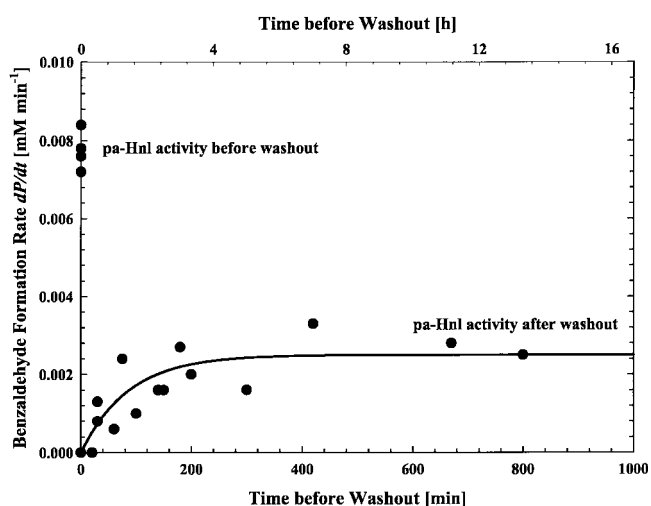


Figure 3. Dependence of the product formation rate, dP/dt , on the adsorption time of pa-Hnl at the DIPE/water interface measured after removal of the aqueous enzyme phase. The solid line corresponds to a best fit to the kinetic model in Equations (1)–(4) with $S = C_{MN} = 10.1 \text{ mM}$, $S_0 = 1.33 \text{ mM}$, $K_m = 14.4 \text{ mM}$, $50 \text{ mM KH}_2\text{PO}_4$ buffer, pH 5.5. After Hickel et al. (2001) with permission.

such as acid, urea, temperature, or pressure. Bulk unfolding processes may be classified as either ‘cooperative’ or ‘noncooperative’ (Dill and Shortle, 1991; Fersht, 1998). In a strongly cooperative unfolding process, the protein structure changes in an ‘all-or-none’ manner. The transition involves only two distinct biological entities: native (N) and unfolded (U) states. Conversely, in a ‘non-cooperative’ transition, several intermediate conformational states become populated having biological activities lying between the extremes represented by the native and unfolded states. Most globular-protein unfolding reactions are well described by a simple two-state cooperative mechanism (Fersht, 1998). Even in cases where the transition proceeds through a series of intermediates, a cooperative process can describe most individual unfolding steps. We consider that enzyme unfolding upon exposure to an interface can be described in a manner similar to that employed for common denaturants in bulk water, such as acid, urea, temperature, or pressure.

With this framework, the enzyme adsorption process and subsequent conformational changes leading to deactivation are illustrated in Figure 4. Rather than tracking a number of intermediate enzyme states at the interface and their individual contributions to the overall measured kinetics, we consider only two states, N and U, having native and (partially) unfolded conformations. These conformations correspond to extremes of enzyme activity and degree of irreversible adsorption at the interface.

Figure 4 depicts the various adsorption events envisioned in our model. At early times, enzyme present in the aqueous phase adsorbs reversibly at the interface in state N with native conformation and activity. Once in this configuration, the enzyme subsequently desorbs into the aqueous phase or is converted into the unfolded state U because of exposure to the interface. Enzyme in state U is significantly unfolded and likely consists of trains and loops extending into the water and organic phases (Anderson et al., 2000; Graham and Phillips, 1979c). State U may have a different projected area than that of state N and is irreversibly adsorbed. Furthermore, in this partially or completely unfolded state, interprotein interactions are enhanced due to exposure of hydrophobic residues (Anderson et al., 2000; Bratko and Blanch, 2001). Adsorbed denatured proteins thus provide sites for further adsorption of native proteins from the underlying aqueous phase with consequent formation of multilayers. Here, we only consider formation of a second protein layer. At long times, the first layer saturates the interface with partially denatured protein, thus contributing less to the overall interfacial catalytic activity. Most of the observed catalytic activity then arises from protein in its native state adsorbed in the second layer.

Interfacial mass balances for enzyme concentrations in the first (1) and second (2) layers involve surface excess

P and S are product and substrate concentrations in the organic phase, k_{cat} is the enzymatic rate constant, a_V is the interfacial area per reactor volume (here $0.1146 \text{ m}^2 \text{ L}^{-1}$), and K_M is the Michaelis-Menten constant (14.4 mM for the interfacial reaction). The last term in parentheses on the right of Equation (4) reflects the Michaelis-Menten linear dependence on enzyme concentration, only now expressed in surface concentrations. We assume that both N and U in layers 1 and 2 contribute to the enzymatic reaction. However, because the U species is partially unfolded, its contribution to the overall rate of product formation is weighted by a parameter ε , set between zero (strong denaturing organic phases such as heptane) to unity (nondenaturing solvents).

The experimental mandelonitrile concentration is 10.1 mM (Hickel et al., 1999). At this concentration, no change in the substrate concentration occurs during the reaction period. Consequently, S is constant in Equation (4). Only the surface coverages depend on time. Thus, given the solution to the enzyme adsorption kinetics described above in Equations (1)–(3), product formation follows directly from integration of Equation (4).

Parameter Determination

The model contains a number of kinetic parameters that we independently evaluate from the experimental data. Figure 3 (i.e., the reaction rate, dP/dt , as a function of time following removal of aqueous-phase enzyme) provides a measure of the U -state enzyme adsorbed in the first layer. At long times, the measured enzyme activity is seen to remain constant. Consequently, we conclude that the first layer of adsorbed protein contains only the U species because the first-layer N species is removed. Accordingly, from Equation (4) the contribution of layer 1 to the long-time reaction rate is:

$$\frac{dP_1^\infty}{dt} = \frac{k_{cat}\Gamma_{\max}a_V}{MW_{pa-Hnl}} \frac{(S - S_0)}{(S - S_0 + K_M)} \varepsilon \quad (5)$$

where $\Gamma_{N1}^\infty = 0$, $\Gamma_{U1}^\infty = \Gamma_{\max}$, and the superscript ∞ denotes infinite time. There are two unknowns in this expression: the product $k_{cat}\Gamma_{\max}$ and ε . From Figure 3, the long-time contribution of denatured enzyme to the overall rate, dP_1^∞/dt , is about $0.0025 \text{ mM min}^{-1}$.

It is now possible to estimate the contribution of the second layer to the total rate of reaction at long times by subtracting the contribution of the first layer, estimated above, from the reaction rates presented in Figure 2. According to Equation (3), at long times the concentration of native enzyme adsorbed in the second layer is related to the aqueous phase enzyme concentration by a Langmuir-type isotherm. Hence, at long times we write that:

$$\frac{dP_2^\infty}{dt} = \frac{k_{cat}a_V}{MW_{pa-Hnl}} \frac{(S - S_0)}{(S - S_0 + K_M)} \Gamma_{N2}^\infty \quad (6)$$

where $\Gamma_{N2}^\infty = c_{pa-Hnl}^\infty \Gamma_{\max} / (c_{pa-Hnl}^\infty + K_2)$ and $K_2 = k_{2D}/k_{2A}$. The unknowns in the above expressions are $k_{cat}\Gamma_{\max}$ and the equilibrium constant K_2 , both of which can be obtained by a fit of the product-formation rate data in Figure 2 to the predictions of Equation (6). With $k_{cat}\Gamma_{\max}$ now available, Equation (5) is employed to estimate ε , the deactivation parameter.

Kinetic data obtained following the removal of aqueous-phase enzyme demonstrate activity decrease within several minutes (Hickel, private communication). Thus, from Equations (1), (3), and (4), we estimate the kinetic rate constants for desorption k_{1D} and k_{2D} each to be approximately 1.0 min^{-1} . In this manner, the kinetic rate constant for adsorption of N_2 molecules in the second layer is estimated as $k_{2A} = K_2 \cdot k_{2D}$. The rate constant of conformational change from N to U , k_C , is directly estimated from the remaining enzyme activity data following removal of the aqueous enzyme phase illustrated in Figure 3. Reversibility is lost in about 180 min. Hence, $k_C = 1/60 \text{ min}^{-1}$ corresponds to conversion of nearly 99% of the N species. This value for the rate constant could also be estimated by examining the dynamic-tension-washout experimental data done under similar conditions (cf., Figs. 10–12 of Hickel et al., 2001).

The only parameter for which no independent estimate is readily available is the kinetic rate constant for adsorption of N molecules in the first layer, k_{1A} . A set of parameters that best fits the product formation for different bulk enzyme concentrations can be obtained from a nonlinear curve-fit of Equations (1)–(4) to the data in Figure 1. Best-fit calculations were performed using Matlab 6.0 (The MathWorks Inc., Natick, MA) with the Optimization Toolbox for nonlinear curve fitting employing multiple data sets. Based on this overall fitting scheme, kinetic rate constants for $pa-Hnl$ at the DIPE/water interface are reported in Table I.

The listed rate constants in Table I reflect individual contributions to the measured enzymatic activity arising from the first layer, in the N and U states, as well as in the second layer, yielding a nearly linear dependence of product concentration with time. These individual contributions, along with the total product production, are graphed in Figure 5 for an enzyme concentration equal to 292 mg L^{-1} . Eventually, the contribution of the N_1 species decays to zero as the native adsorbed protein decays to the U_1 unfolded state finally occupying complete coverage. Likewise, the contribution to product formation of the second layer eventually reaches a constant due to reversible adsorption at U_1 sites. In Figure 5, the loss of activity due to unfolding in the first layer (N to U transition) is nearly compensated by the additional activity arising from development of the second adsorbed enzyme layer. Departure from constant rates of product formation at longer times is physically expected, as some denaturation must occur in the second

Table I. Kinetic parameters.

Symbol	Value	Units
k_{1A}	5.23×10^{-2}	$\text{L min}^{-1} \text{mg}^{-1}$
k_{1D}	1.0	min^{-1}
k_{2A}	1.02×10^{-2}	$\text{L min}^{-1} \text{mg}^{-1}$
k_{1D}	1.0	min^{-1}
k_C	0.0167	min^{-1}
$k_{cat}\Gamma_{\max}$	3.20×10^4	$\text{mg m}^{-2} \text{min}^{-1}$
ε	0.13	[-]

layer. Deactivation of the second layer is not included in our model, because pa-Hnl is extremely stable at the DIPE/water interface up to several hours, and no apparent overall loss of activity is detected over the time scale of our experiments. Thus, the linear kinetics observed in Figure 1 is not the result of a stable, reversibly adsorbing native enzyme, but rather a more complicated combination of factors including unfolding, denaturing, and irreversible and multilayer adsorption. Other more apolar solvents than DIPE that strongly adsorb and denature pa-Hnl are not expected to demonstrate such simple linear kinetics, and indeed they do not (Hickel et al., 2001).

Comparison to Experiment

As noted earlier, solid lines in Figures 1–3 are the result of the proposed kinetic model using the parameters listed in Table I. Excellent agreement is obtained in Figure 1 demonstrating a linear product appearance in time spanning 2 orders of magnitude in enzyme concentration. Likewise, agreement of theory with the re-

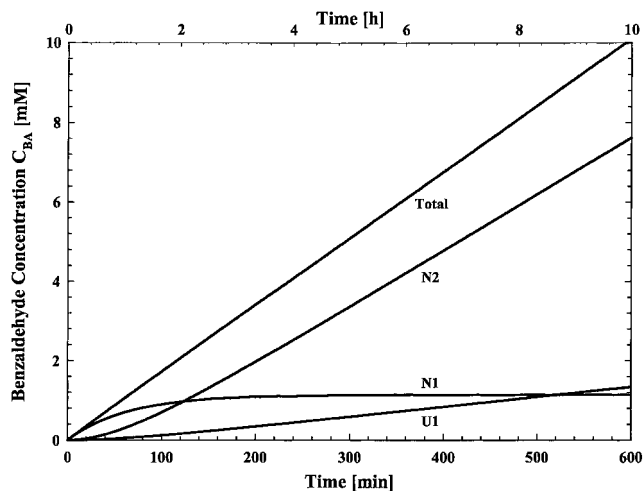


Figure 5. Dependence of benzaldehyde product formation, ($C_{BA} = P$) on time, for a pa-Hnl aqueous-phase concentration: $c_{pa-Hnl}^{\infty} = 292 \text{ mg L}^{-1}$, $50 \text{ mM KH}_2\text{PO}_4$, pH 5.5, $C_{MN} = 10.1 \text{ mM}$. The uppermost solid line corresponds to the kinetic model in Equations (1)–(4) using the parameters in Table I. The remaining solid lines indicate individual contributions to the overall measured reaction rate arising from molecules in either the native N or unfolded U states of the first layers, and molecules in the native state N in the second layer.

action-rate isotherm (i.e., the slopes of the product formation curves in Fig. 1) in Figure 2 is quite good. Originally, we ascribed the limiting behavior in Figure 2 as due to a reversible Langmuir-like adsorption of pa-Hnl at the DIPE/water interface (Hickel et al., 1999). The current kinetic model reflects irreversible adsorption and denaturing of pa-Hnl at the DIPE/water surface.

Finally, agreement of the kinetic model with the washout kinetic data in Figure 3 is again excellent. This curve cannot be explained without invoking enzyme partial denaturation and irreversible adsorption (Hickel et al., 2001). Our proposed kinetic model captures these two essential features.

Discussion of Kinetic Results

The enzymatic-activity data presented in Figure 3 following washout of the aqueous enzyme clearly demonstrate that some irreversible adsorption has occurred after about 3 h. As previously reported, this loss of reversibility parallels interfacial-tension measurements under similar conditions (see Figs. 10–12 of Hickel et al., 2001). At longer times, about 25–30% of the initial enzymatic activity level is observed. We account for partially reversible enzyme adsorption by incorporating a reversibly adsorbed and catalytically active second protein layer. Partial reversibility is also obtained with a single-layer size-change model (Brusatori and Van Tassel, 1999). In this alternate model, a transition from native to irreversibly adsorbed state is considered to involve a protein-spreading mechanism resulting in a size increase of the irreversibly adsorbed species. In the spreading mechanism, partial reversibility evolves at close to saturation coverages when there is no further space available for spreading. As a consequence, reversibly adsorbed molecules in their native state are blocked from unfolding to an irreversibly adsorbed configuration. Unfortunately, such a steric-hindrance mechanism cannot explain the interfacial-tension measurements reported earlier that indicate total loss of reversibility of the first protein layer within 3 h (see Figs. 10–12 of Hickel et al., 2001).

The kinetic rate constants for adsorption obtained from a fit to the data indicate that the adsorption rate into the first layer, characterized by k_{1A} , is about 5 times faster than adsorption into the second layer, characterized by k_{2A} . From our model, it is not possible to obtain the individual values of either k_{cat} or Γ_{\max} but only their product $k_{cat}\Gamma_{\max}$ which has a value of $32,000 \text{ m}^2 \text{ mg}^{-1} \text{ min}^{-1}$. Using a projected area based on the diameter of pa-Hnl and assuming hexagonal close packing at the interface, a value of Γ_{\max} is estimated to be 1.20 mg m^{-2} (Hickel et al., 1999). It then follows that the catalytic rate constant for the native state k_{cat}^N is $26,600 \text{ min}^{-1}$ (443 s^{-1}) and for the unfolded-state rate constant $k_{cat}^U = \varepsilon \cdot k_{cat}^N$, is $3,466 \text{ min}^{-1}$ (58 s^{-1}). Compared to the catalytic rate constant in the aqueous bulk phase of

11,520 min⁻¹ (192 s⁻¹) (Hickel et al., 1999), the specific interfacial enzyme activity is higher upon initial adsorption at the interface, and is followed by deactivation as a consequence of unfolding. Small conformational changes of lipases have been proposed as the origin of this enhanced activity at the interface (Hickel et al., 1999). Partial unfolding may, to some extent, favor substrate binding and conversion. The deactivation parameter ε has a value of 0.13 in Table I, indicating that U molecules are significantly less active than the reversibly adsorbed N species, even with DIPE as the organic solvent.

First-order kinetics has been employed to describe the unfolding process. As noted earlier, noncooperative unfolding processes involve several intermediates and are usually described by second-order kinetics (Dill and Shortle, 1991). *Hevea brasiliensis*, is similar to pa-Hnl, and has been reported to unfold in aqueous buffer as a function of acid denaturant in a noncooperative manner (Hanefeld et al., 2001). A similar description of second-order pa-Hnl unfolding at the interface could have been employed in this work. The essential conclusions of this article, however, remain unchanged by assuming a simple first-order process.

The proposed interfacial kinetic framework easily lends itself to description of the effects of other solvents. For the case of heptane, a highly denaturing solvent, we expect an initially high rate, characterized by a catalytic rate constant for the adsorbed native state (k_{cat}^N) which is much higher than that in the bulk aqueous phase, followed by a rapid deactivation as no enzyme activity is detected at later times (i.e., $\varepsilon = 0$). Enzymes adsorbed in a second layer will also deactivate. This explains the burst in kinetics accompanied by rapid deactivation illustrated in Figure 6 of Hickel et al. (2001).

DYNAMIC INTERFACIAL TENSION

Dynamic Interfacial Enzyme Activity

Dynamic-interfacial-tension measurements provide additional insight into both the adsorption mechanisms and the subsequent conformational rearrangement processes that take place at the fluid/fluid interface. Measured dynamic interfacial tensions typically display three time regimes (Beverung et al., 1998; 1999; Tripp et al., 1995). The first regime is the lag time commonly associated with the rate of arrival of proteins at the interface from the aqueous phase following a mass-transfer mechanism

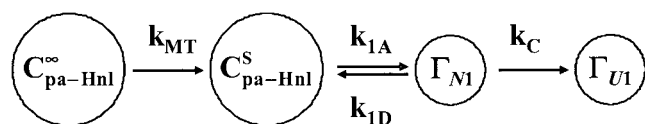


Figure 6. Schematic of the individual mass transfer and kinetic events associated with the onset of unfolding in the first layer.

that can be convective, diffusive, or a combination of both. During this period, there is minimal reduction in tension. This slight reduction in tension is usually interpreted as due to a sparsely populated interface (Beverung et al., 1999). The second regime indicates initial unfolding of protein molecules at the interface entailing exposure and/or protrusion of protein segments into the air or organic phases accompanied by a pronounced decrease in interfacial tension. The third time regime provides further lowering in tension by strong lateral interactions among adsorbed proteins, resulting in, for example, the formation of interfacial aggregates or a gel. This mechanism reduces tension at a slower rate than that occurring in the second time regime. This last regime is seldom observed for globular proteins even over time scales up to a day. In contrast, loosely bound, random coil proteins, like β -casein exhibit this third regime comparatively quickly at ambient temperature.

Examination of the experimental lag time, especially its deviation from values resulting from mass-transfer limitations, provides insight into the time scale of enzyme denaturation at an interface, especially with respect to the nature of the solvent. Here we consider that interfacial-tension lowering is mainly caused only by molecules adsorbed in the first layer and is primarily due to enzymes in the unfolded state. The lag time then provides a measure of the time scale for arrival of N species at the interface followed by conversion to the U state.

As illustrated in Figure 6, consider an enzyme adsorbing from solution in the native state followed by conformational change to the unfolded state. The aqueous-phase bulk enzyme concentration directly at the interface is denoted as c_{pa-Hnl}^S . Bulk aqueous enzymes at this location are considered to be in equilibrium with those reversibly adsorbed in the native state at the interface with surface concentration Γ_{N1} . Following exposure to the interface, the adsorbed enzymes unfold in the sequence of steps shown in Figure 6. In this sequence, the second, or adsorption, event is reversible and is replaced by an irreversible step with an effective rate constant designated as k' (Cleland, 1963):

$$k' = \left(\frac{k_C}{k_C + k_{1D}} \right) k_{1A} (\Gamma_{\max} - \Gamma_{N1} - \Gamma_{U1}) c_{pa-Hnl}^S \quad (7)$$

where the first term in parentheses denotes the probability of the native adsorbed species unfolding rather than desorbing. The total characteristic time required to reach the unfolded state also includes a mass-transfer resistance and a kinetic resistance to unfold. Hence, the total lag time is given by the sum of three transit times:

$$\tau_{lag} = \frac{1}{a\gamma k_{MT}} + \frac{\Gamma_{\max}}{k'} + \frac{1}{k_C} \quad (8)$$

where k_{MT} denotes a mass-transfer coefficient. The first term on the right corresponds to the characteristic mass-transfer time for bringing a protein from the bulk to a sublayer immediately adjacent to the interface. The second term corresponds to the characteristic time for adsorption of the native species: It is a measure of the protein affinity for the organic/water interface. The last term corresponds to the characteristic time for conformational rearrangement once adsorbed.

In a typical pendant-drop interfacial-tension measurement in the absence of stirring, the mass-transfer resistance is typically due to diffusion, assuming negligible natural convection. A diffusive time-scale for transport to the interface is found from the characteristic diffusive length, given by the ratio of the maximum possible adsorbed amount Γ_{\max} to that available in the bulk c_{pa-Hnl}^{∞} , and the native-state protein bulk diffusion coefficient, D . With these definitions, Equation (8) becomes:

$$\tau_{lag} \cong \frac{1}{D} \left(\frac{\Gamma_{\max}}{c_{pa-Hnl}^{\infty}} \right)^2 + \frac{k_C + k_{1D}}{k_C k_{1A} c_{pa-Hnl}^S} + \frac{1}{k_C} \quad (9)$$

By considering a typical protein diffusion coefficient of $D \sim 5 \times 10^{-7} \text{ cm}^2 \text{ s}^{-1}$, Γ_{\max} equal to 1–2 mg m^{-2} , and $c_{pa-Hnl}^{\infty} = 10 \text{ mg L}^{-1}$, we estimate the diffusion time scale to be about 100 s.

Interfacial-tension lowering only becomes appreciable for surface concentrations of the tension-lowering species, i.e., the unfolded state, above 90% coverage, because interfacial-tension lowering in a site-model scales as $\ln[(\Gamma_{\max} - \Gamma_{U1})/\Gamma_{\max}]$. Hence, a more reasonable estimate of the interfacial tension lag time is within a multiple of 4–5 times τ_{lag} . Lag times are further under-predicted by Equation (9), because the coverage-dependence term $(\Gamma_{\max} - \Gamma_{N1} - \Gamma_{U1})$ that multiplies k_{1A} has been estimated for simplicity as Γ_{\max} .

Lag Times

For strongly denaturing solvents where pa-Hnl exhibits a high adsorption affinity (i.e., a high k_{1A} and a small k_{1D}) and a propensity for unfolding (i.e., high k_C), the lag times in a tension measurement are limited by enzyme diffusion to and from the interface. This time scale is given by the first term on the right of Equation (9). This is indeed the case for the solvent heptane, as previously observed by Hickel et al., for which tension lowering is almost immediately observed, accompanied by a very fast loss of enzymatic activity (see Fig. 8 of Hickel et al., 2001).

For more weakly denaturing solvents, the affinity for the interface is lower (i.e., a small k_{1A} and a high k_{1D}) as well as is the propensity for unfolding (i.e., a small k_C). Here the lag times observed are considerably longer than estimated for diffusion alone and are controlled by a combination of adsorption and conformational rear-

rangements at the interface. In this limiting case, Equation (9) reduces to:

$$\tau_{lag} \cong \frac{k_C + k_{1D}}{k_C k_{1A} c_{pa-Hnl}^{\infty}} + \frac{1}{k_C} \quad (10)$$

This second case applies to DIPE as the organic phase. No appreciable lowering in tension is observed for up to 15 h for an aqueous enzyme concentration equal to 10 mg L^{-1} . Concomitantly, no significant enzyme deactivation is observed for several hours indicating a slow transition to the unfolded, less-active state (see Fig. 8 of Hickel et al., 2001). The observed lag time with dibutyl ether (DBE) is intermediate between DIPE and heptane, which is in agreement with the observed activities.

It is also instructive to compare adsorption of β -casein, lysozyme, and pa-Hnl at the DIPE interface all at the same concentration (see Fig. 13 of Hickel et al., 1999). The small differences in protein diffusion coefficients cannot explain the large variation of the observed lag times. β -casein, being a coil-like protein, quickly reduces tension after a few seconds. Lysozyme, being globular, exhibits a long lag time up to 100 min, indicating a lower proclivity for interfacial unfolding. No appreciable lowering in tension due to pa-Hnl is observed even after 15 h at an aqueous enzyme concentration equal to 10 mg L^{-1} indicating slow arrival to the unfolded state. The prevalent mechanism dictating such long lag times, e.g., weak adsorption or slow unfolding, cannot be answered solely on the basis of interfacial-tension measurements. Measurements of adsorbed amounts under the same conditions, for instance using ellipsometry or TIRFS, are also required (Graham and Phillips, 1979b; Tupy et al., 1998).

CONCLUSIONS

The kinetic model developed in this work confirms our previous conclusions while providing additional quantitative insight into the reaction kinetics of pa-Hnl at the DIPE/water interface (Hickel et al., 1999; 2001). Upon adsorption at the organic solvent/water interface, pa-Hnl likely denatures and deactivates. Exposure of an enzyme to an interface acts in much the same way as exposure to denaturants commonly used in bulk unfolding/refolding studies. The adsorbed protein molecule undergoes conformational change and rearrangement at the interface accompanied by a reduction in catalytic activity. This is true even for the DIPE/water interface for which no apparent loss of activity can be measured within the several hours of the experiments undertaken. As the adsorbed enzymes unfold and deactivate in the layer immediately adjacent to the interface, they act as seeds for multilayer growth (taken into account here as a second layer) due to attractive intermolecular interactions, probably arising from exposure of their hydrophobic cores at the interface. For the case of the DIPE/water interface, however,

this unfolding does not compromise the overall measured reaction rate that remains constant within the duration of our experiments. Apparently, partial deactivation of pa-Hnl adsorbed in the first layer is offset by the catalytic contribution of native pa-Hnl adsorbed in the sublayer. Because of denaturation, some irreversibility develops already after short times, about 20 minutes. Partial reversibility is obtained at large times as a consequence of multilayer formation. This reversibility cannot be detected by dynamic-tension washout experiments because surface tension is primarily a probe of the energetic state of molecules adsorbed in the first layer. However, it is detectable by enzymatic-activity washout experiments.

The extraordinary stability of pa-Hnl at the DIPE/water interface arises from the duration of this 'overall compensation' mechanism being rather long, comparable to the time-scale of our experiments and is responsible for the nearly linear product formation with time. At longer times than measured, we anticipate that the catalytic activity of pa-Hnl should diminish. Interfacial denaturation appears to be a rather general phenomenon. For the case of more apolar, strongly denaturing solvents, the end of this 'overall compensation' regime is observed much earlier as in the case of heptane and DBE as the organic solvents.

The framework of our kinetic model is particularly useful for the interpretation of dynamic-tension lag times. A measured lag time greater than that predicted based on mass-transfer considerations is an indication of either strong kinetic adsorption barriers and/or of a slow propensity to unfold. It is not possible to determine the prevailing mechanism without an accompanying measure of the interfacial adsorbed amounts. In the event of long lag times, one can expect the enzyme to display a small but stable catalytic activity for extended periods of time at the organic solvent/buffer interface, as in the case of DIPE. Dynamic-tension measurements are thus an invaluable tool for a rational approach to solvent selection and enzyme engineering.

NOMENCLATURE

a_V	interfacial area to reactor volume ratio [$\text{m}^2 \text{L}^{-1}$]
c_{pa-Hnl}^∞	pa-Hnl concentration in the aqueous bulk phase [mg L^{-1}]
c_{pa-Hnl}^S	pa-Hnl concentration at DIPE/aqueous interface vicinity [mg L^{-1}]
C_{BA}	benzaldehyde concentration [mM]
C_{MN}	mandelonitrile concentration [mM]
D	pa-Hnl diffusion coefficient [$\text{cm}^2 \text{s}^{-1}$]
DBE	dibutyl ether
DIPE	diisopropyl ether
Hnl	hydroxynitrile lyase
k'	effective irreversible rate constant [$\text{mg m}^{-2} \text{min}^{-1}$]
k_{1A}	rate constant of protein adsorption in first layer in native state [$\text{L mg}^{-1} \text{min}^{-1}$]
k_{1D}	rate constant of protein desorption in first layer in native state [$\text{mg}^{-1} \text{min}^{-1}$]

k_{2A}	rate constant of protein adsorption in second layer in native state [$\text{L mg}^{-1} \text{min}^{-1}$]
k_{2D}	rate constant of protein desorption in first layer in native state [min^{-1}]
k_C	rate constant of protein unfolding at the interface [min^{-1}]
k_{cat}	catalytic rate constant [min^{-1}]
k_{MT}	mass transfer characteristic rate constant [$\text{L m}^{-2} \text{min}^{-1}$]
K_2	k_{2A}/k_{2D}
K_M	Michaelis-Menten constant [mM]
MTBE	methyl tert-butyl ether
MW_{pa-Hnl}	pa-Hnl molecular weight [kg mol^{-1}]
P	product (benzaldehyde) concentration [mM]
pa-Hnl	hydroxynitrile lyase from <i>Prunus amygdalus</i> (almond)
S	substrate (mandelonitrile) concentration [mM]
S_0	initial substrate concentration [mM]
ε	deactivation parameter [–]
Γ_{N1}	interfacial enzyme concentration in native state and first layer [mg m^{-2}]
Γ_{U1}	interfacial enzyme concentration in denatured state and first layer [mg m^{-2}]
Γ_{N2}	interfacial enzyme concentration in native state and second layer [mg m^{-2}]
Γ_{max}	maximal interfacial enzyme concentration [mg m^{-2}]
τ_{lag}	lag time for appearance of unfolded state [min]

References

- Anderson RE, Pande VS, Radke CJ, 2000. Dynamic lattice Monte Carlo simulation of a model protein at an oil/water interface. *J Chem Phys* 112:9167–9185.
- Bauer M, Griengl H, Steiner W, 1999. Parameters influencing stability and activity of a (S)-hydroxynitrile lyase from *Hevea brasiliensis* in two-phase systems. *Enzyme Microb Technol* 24:514–522.
- Beverung CJ, Radke CJ, Blanch HW, 1998. Adsorption dynamics of (L)-glutamic acid copolymers at a heptane/water interface. *Biophys Chem* 70:121–132.
- Beverung CJ, Radke CJ, Blanch HW, 1999. Protein adsorption at the oil/water interface: Characterization of adsorption kinetics by dynamic interfacial tension measurements. *Biophys Chem* 81:59–80.
- Bratko D, Blanch HW, 2001. Competition between protein folding and aggregation: A three-dimensional lattice-model simulation. *J Chem Phys* 114:561–569.
- Brusatori MA, Van Tassel PR, 1999. A kinetic model of protein adsorption/surface-induced transition kinetics evaluated by the scaled particle theory. *J Colloid Interface Sci* 219:333–338.
- Cascão Pereira LG, Johansson C, Blanch HW, Radke CJ, 2001. A bike-wheel microcell for measurement of thin-film forces. *Colloids Surf A* 186:103–111.
- Cleland WW, 1963. Kinetics of enzyme-catalyzed reactions with 2 or more substrates or products 1. Nomenclature and rate equations. *Biochim Biophys Acta* 67:104–172.
- Dill KA, Shortle D, 1991. Denatured states of proteins. *Annu Rev Biochem* 60:795–825.
- Dreveny I, Gruber K, Glieder A, Thompson A, Kratky C, 2001. The hydroxynitrile lyase from almond. A lyase that looks like an oxidoreductase. *Structure* 9:803–15.
- Effenberger F. 1994. Synthesis and reactions of optically active cyanohydrins. *Angew Chem Int Ed Engl* 33:555–564.
- Effenberger F, Förster S, Wajant H. 2000. Hydroxynitrile lyases in stereoselective catalysis. *Curr Opin Biotechnol* 11:532–539.

- Erickson JS, Sundaram S, Stebe KJ. 2000. Evidence that the induction time in the surface pressure evolution of lysozyme solutions is caused by a surface phase transition. *Langmuir* 16:5072–5078.
- Fainerman VB, Miller R, Wustneck R, Makievski AV. 1996. Adsorption isotherm and surface tension equation for a surfactant with changing partial molar area I. Ideal surface layer. *J Phys Chem* 100:7669–7675.
- Fersht A. 1998. *Structure and mechanism in protein science*, 1st ed. New York: W.H. Freeman. p 518–521.
- Förster S, Roos J, Effenberger E, Wajant H, Sprauer A. 1996. The first recombinant hydroxynitrile lyase and its application in the synthesis of (S)-cyanohydrins. *Angew Chem Int Ed Engl* 35:437–439.
- Graham DE, Phillips MC. 1979a. Proteins at liquid interfaces. I. Kinetics of adsorption and surface denaturation. *J Colloid Interface Sci* 70:403–414.
- Graham DE, Phillips MC. 1979b. Proteins at liquid interfaces. II. Adsorption isotherms. *J Colloid Interface Sci* 70:415–426.
- Graham DE, Phillips MC. 1979c. Proteins at liquid interfaces. III. Molecular structures of adsorbed films. *J Colloid Interface Sci* 70:427–439.
- Hanefeld U, Stranzl G, Straathof AJJ, Heijnen JJ, Bergmann A, Mittelbach R, Glatter O, Kratky C. 2001. Electrospray ionization mass spectrometry, circular dichroism and SAXS studies of the (S)-hydroxynitrile lyase from *Hevea brasiliensis*. *Biochim Biophys Acta* 1544:133–142.
- Haynes CA, Norde W. 1995. Structures and stabilities of adsorbed proteins. *J Colloid Interface Sci* 169:313–328.
- Hickel A, Graupner M, Lehner D, Hermetter A, Glatter O, Griengl H. 1997. Stability of the hydroxynitrile lyase from *Hevea brasiliensis*: A fluorescence and dynamic light scattering study. *Enzyme Microb Technol* 21:361–366.
- Hickel A, Hasslacher M, Griengl H. 1996. Hydroxynitrile lyases: Functions and properties. *Physiol Plant* 98:891–898.
- Hickel A, Radke CJ, Blanch HW. 1998. Hydroxynitrile lyase adsorption at liquid/liquid interfaces. *J Mol Catalysis B Enzymatic* 5:349–354.
- Hickel A, Radke CJ, Blanch HW. 1999. Hydroxynitrile lyase at the diisopropyl ether/water interface: Evidence for interfacial enzyme activity. *Biotechnol Bioeng* 65:425–436.
- Hickel A, Radke CJ, Blanch HW. 2001. Role of organic solvents on pa-hydroxynitrile lyase interfacial activity and stability. *Biotechnol Bioeng* 74:18–28.
- Johnson DV, Zabelinskaja-Mackova AZ, Griengl H. 2000. Oxynitri- lases for asymmetric C-C bond formation. *Curr Opin Chem Biol* 4:103–109.
- Kiljunen E, Kanerva LT. 1997a. Approach to (R)- and (S)-ketone cyanohydrins using almond and apple meal as a source of (R)- oxynitrilase sources for the synthesis of cyanohydrins in diiso- propyl ether. *Tetrahedron-Assymetry* 8:1551–1557.
- Kiljunen E, Kanerva LT. 1997b. Novel (R)-oxynitrilase sources for the synthesis of (R)-cyanohydrins in diisopropyl ether. *Tetrahedron- Assymetry* 8:1225–1234.
- Loos WT, Geluk HW, Ruijken MMA, Kruse CG, Brussee J, van der Gen A. 1995. Synthesis of optically active cyanohydrins using (R)- oxynitrilase in a liquid/liquid biphasic system. I. An industrially useful procedure. *Biocatal Biotrans* 12:255–266.
- Malmsten M. 1998. *Biopolymer at Interfaces*. New York: Marcel Dekker. p 562–588.
- Park K, Mersny R. 2000. *Controlled drug delivery*. Washington, DC: American Chemical Society.
- Stuart MAC, Fleer GJ, Lyklema J, Norde W, Scheutjens J. 1991. Adsorption of ions, polyelectrolytes and proteins. *Adv Colloid Interface Sci* 34:477–535.
- Tripp BC, Magda JJ, Andrade JD. 1995. Adsorption of globular proteins at the air/water interface as measured via dynamic surface tension—concentration dependence, mass-transfer con- siderations, and adsorption kinetics. *J Colloid Interface Sci* 173: 16–27.
- Tupy M. 1998. Protein adsorption dynamics at the oil/water interface as studied by total internal reflection fluorescence spectroscopy. Ph.D. thesis, University of California at Berkeley.
- Tupy MJ, Blanch HW, Radke CJ. 1998. Total internal reflection flu- orescence spectrometer to study dynamic adsorption phenomena at liquid/liquid interfaces. *Ind Eng Chem Res* 37:3159–3168.
- Wahlgren M, Arnebrant T, Lundstrom I. 1995. The adsorption of lysozyme to hydrophilic silicon oxide surfaces—comparison be- tween experimental data and models for adsorption kinetics. *J Colloid Interface Sci* 175:506–514.
- Wajant H, Effenberger F. 1996. Hydroxynitrile lyases of higher plants. *Biol Chem* 377:611–617.
- Willeman WF, Hanefeld U, Straathof AJJ, Heijnen JJ. 2000. Estima- tion of kinetic parameters by progress curve analysis for the synthesis of (R)-mandelonitrile by *Prunus amygdalus* hydroxynit- rile lyase. *Enzyme Microb Technol* 27:423–433.